

**RETRIEVING MORE ELEMENTS FROM DAWN'S GAMMA RAY SPECTROMETER.** N. Yamashita<sup>1</sup>, T. H. Prettyman<sup>1</sup>, and R. C. Reedy<sup>1</sup>, <sup>1</sup>Planetary Science Institute (1700 East Fort Lowell, Suite 106, Tucson, AZ 85719, yamashita@psi.edu).

**Introduction:** The Gamma Ray and Neutron Detector (GRaND) of NASA's Dawn mission has mapped the surface elemental composition of the asteroid 4 Vesta, providing new insights into processes underlying its formation and evolution. First results from the low-altitude mapping orbit (LAMO) of Vesta were reported elsewhere by [1-5].

Within a couple of body radii, GRaND is sensitive to neutron and gamma ray emissions from planetary surfaces. A detailed description of the GRaND instrument, data processing, and archiving is described in [6] and in documents accompanying the archived data in the Planetary Data System (PDS) at the Small Bodies Node. Here, we provide a brief overview of the processing steps necessary to produce higher level gamma ray spectroscopy products that are required for further elemental analyses of Vesta. This study builds upon previously reported work of [1,5-7].

**Observation Phases:** Prior to arrival at Vesta, GRaND conducted an initial check out (ICO) in interplanetary space and further testing during Mars Gravity Assist (MGA). During encounter with Vesta, GRaND measured gamma rays and neutrons at various distances from Vesta: >>3000 km (Vesta Science Approach, VSA), 3000 km (Survey), 950 km (high altitude mapping orbit, HAMO), and 475 km in LAMO.

Planetary nuclear spectroscopy requires long accumulation times for a statistically meaningful observation. During each observation phase, the gain of the detector signal changed continuously depending on various factors, such as detector settings, galactic and solar cosmic ray fluxes, and temperature (Fig. 1). Such temporal gain shifts result in the degradation of the

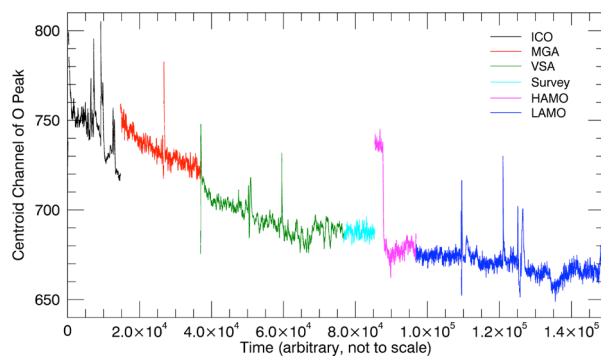


Fig. 1 Temporal variation of the peak centroid of the 6.1-MeV gamma rays from oxygen observed by the BGO detector in GRaND. Each color-coded observation phase is not necessarily consecutive, because of transition phases which are not shown. See text for abbreviations.

energy resolution as well as the signal-to-background ratio when many spectra are combined over long time intervals. In order to recover the intrinsic resolution of the detector and achieve maximum elemental sensitivity, the following data reduction steps have been applied to the PDS Level 1A data products. The new products will be submitted and subsequently released as Level 1B dataset in PDS following peer review.

#### Data Reduction Steps Needed to Produce Higher Level Products:

**Detection of Peak Centroids.** Peak centroids of five major gamma-ray peaks found in the BGO spectrum, namely at 0.478 MeV from <sup>10</sup>B, 0.511 MeV from positron annihilation, 2.2 MeV from <sup>27</sup>Al, 4.4 MeV from <sup>12</sup>C, and 6.1 MeV from <sup>16</sup>O have been monitored for all of the time-series spectra using the second-derivative peak identification method of [8]. The centroid for the O peak is shown in Fig. 1. Despite using the same high voltage setting throughout the mission, the gain has decreased by more than 10% since ICO.

**Removal of Bad Events.** The temporal variation of gain clearly indicates events that are not suitable for elemental observation, such as solar particle events (sharp spikes in Fig. 1) and short periods of time when the instrument was not fully configured. Together with scaler data [6], those "bad" events were flagged so that users of higher level spectra can easily remove them when it is necessary to do so based on their interests.

**Gain Correction and Energy Calibration.** The temporal variations of the peak centroids were fitted against their reference energies to correct all of the spectra to the same gain and offset. Several fitting schemes have been tried and we concluded that a quadratic regression between the peak centroids and the reference energies give the smallest absolute deviation

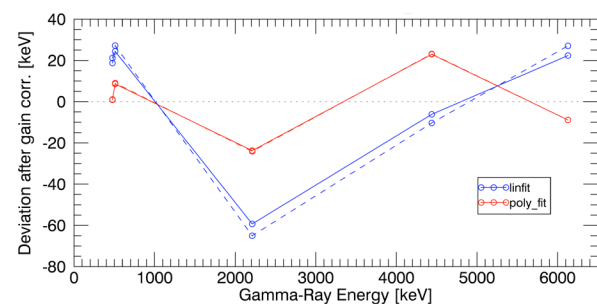


Fig. 2 Deviation of peak centroids from reference energies after gain correction. Solid lines indicate LAMO and dashed lines indicate VSA. Gain correction by linear regression is in blue and quadratic in red.

of the peak energies as well as the smallest relative deviation among the observation phases (Fig. 2). Since gain is expected to change relatively slowly, the spectra were smoothed with a moving average of  $\sim 5$  hours or about one orbital period of LAMO. Then, using the regression curve, the uncorrected channel counts were converted to corrected channel counts having equivalent energies of  $8.9 \times$  channel number in keV [6,9-12].

**Difference Spectrum:** Since the BGO detector cannot spectrally resolve many of gamma-ray peaks of interest, and gamma-ray emission from the spacecraft is significant, it is crucial to reduce the background for the elemental analyses. We used data acquired far from Vesta in VSA as a background spectrum, and created a difference spectrum by subtracting the total VSA spectrum from the total LAMO spectrum. As a result, the difference spectrum should contain signals that originate primarily from the vestan surface.

**Peak-Width Correction.** When taking the difference of two spectra, not only gain but also their peak widths have to be equal to avoid the introduction of artifacts. Our careful peak analyses show that the widths of major peaks in LAMO and VSA spectra can be well characterized by the square root of gamma-ray's energies, with an offset of  $\sim 20$  ch (Fig. 3). The exception was the annihilation peak, probably due to its extremely high and steep continuum. Because resolution varies with energy, we convolved each spectrum with an energy-dependent function, such that all spectra had the same energy resolution. The target width of convolution (shown in Fig. 3) was determined such that it exceeds widths of both the LAMO and VSA spectra. This results in an artifact-free difference spectrum, with peak widths consistent with the LAMO and VSA spectra. The target width of 6% wider than the LAMO spectrum trend was used in this study (Fig.3). The resulting difference spectrum is shown in Fig. 4.

**Retrieving More Elements:** Gamma-ray peaks in the difference spectrum were analyzed using the GRAND Peak Analysis Widget [6]. Using peak fitting (see Fig. 4), we were able to identify and quantify the

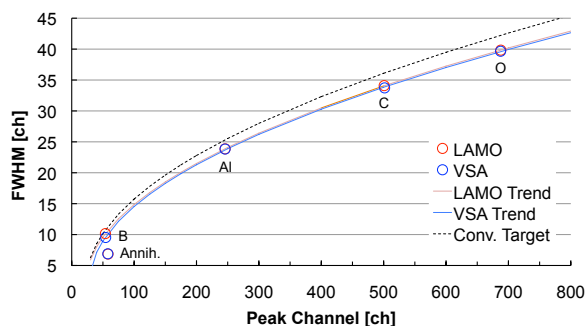


Fig. 3 Widths of the five major peaks and their trend lines scaled with the square root of energies.

counting rates for many gamma rays that were otherwise not detectable with the Level 1A spectra [e.g., see 13]. Previous studies focused on strong peaks from Fe, Si, and O [1,5] as well as the high energy gamma ray continuum [3]. We expect that improvements in data reduction described here and the application of spectral unmixing algorithms [14] will enable accurate quantification of additional elements, such as Al, Mg, K, Th, and possibly Ni.

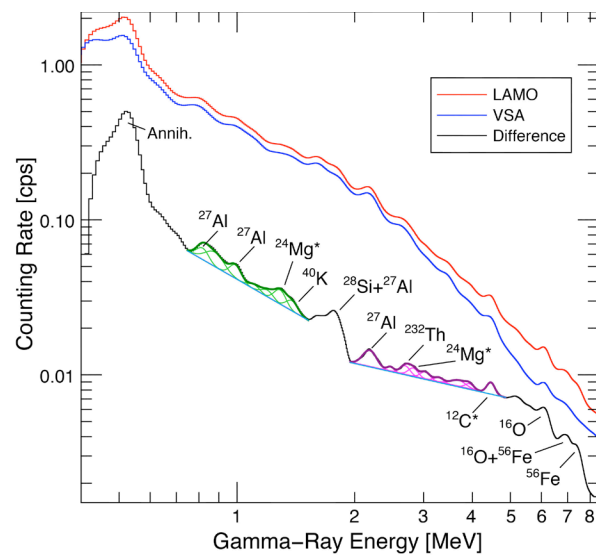


Fig. 4 Gain- and width-corrected spectra for LAMO and VSA and the derived difference spectrum. Some of the prominent peaks are fitted and/or labeled.

**Acknowledgement:** This work was funded by the NASA Dawn mission and Dawn at Vesta Participating Scientist program (RCR). Contributions by members of the Dawn Science, Spacecraft and Instrument-Operations teams at JPL and UCLA are greatly appreciated.

**References:** [1] Prettyman T.H. et al. (2012) *Science*, 338, 242-246. [2] Lawrence D.J. et al. (2013) *MAPS*, 48, 2271-2288. [3] Peplowski P.N. et al. (2013) *MAPS*, 48, 2252-2270. [4] Prettyman T.H. et al. (2013) *MAPS*, 48, 2211-2236. [5] Yamashita N. et al. (2013) *MAPS*, 48, 2237-2251. [6] Prettyman T.H. et al. (2011) *Space Sci. Rev.*, 163, 371-459. [7] Yamashita N. et al. (2012) *LPS XLIII*, Abstract #2448. [8] Mariscotti M.A. (1967) *Nuc. Inst. Methods* 50, 309-320. [9] Lawrence D.J. et al. (2004) *JGR* 109, E07S05. [10] Prettyman et al. (2004) *JGR* 109, E05001. [11] Prettyman T. H. et al. (2004) Mars 2001 Odyssey Neutron Spectrometer processing. NASA PDS. [12] Prettyman T.H. and Feldman W.C. (2012) PDS data processing Gamma Ray and Neutron Detector. NASA PDS. [13] Prettyman T.H. et al, this meeting. [14] Prettyman T. H. (2006) *JGR*, 111, E12007.